

Northumbria Research Link

Citation: Wang, Zhiguo, Li, Zhijie and Fu, Yong Qing (2017) Composites of Piezoelectric Materials and Silicon as Anode for Lithium Ion Batteries. ChemElectroChem. ISSN 2196-0216

Published by: Wiley-Blackwell

URL: <http://dx.doi.org/10.1002/celec.201700043>
<<http://dx.doi.org/10.1002/celec.201700043>>

This version was downloaded from Northumbria Research Link:
<http://nrl.northumbria.ac.uk/id/eprint/30181/>

Northumbria University has developed Northumbria Research Link (NRL) to enable users to access the University's research output. Copyright © and moral rights for items on NRL are retained by the individual author(s) and/or other copyright owners. Single copies of full items can be reproduced, displayed or performed, and given to third parties in any format or medium for personal research or study, educational, or not-for-profit purposes without prior permission or charge, provided the authors, title and full bibliographic details are given, as well as a hyperlink and/or URL to the original metadata page. The content must not be changed in any way. Full items must not be sold commercially in any format or medium without formal permission of the copyright holder. The full policy is available online: <http://nrl.northumbria.ac.uk/policies.html>

This document may differ from the final, published version of the research and has been made available online in accordance with publisher policies. To read and/or cite from the published version of the research, please visit the publisher's website (a subscription may be required.)



**Northumbria
University**
NEWCASTLE



UniversityLibrary

Composites of Piezoelectric Materials and Silicon as Anode for

Lithium Ion Batteries

Zhiguo Wang,^{1*} Zhijie Li,¹ Yong Qing Fu^{1,2*}

1 School of Physical Electronics, Center for Public Security Information and Equipment Integration Technology, University of Electronic Science and Technology of China, Chengdu, 610054, P.R. China

2 Faculty of Engineering and Environment, University of Northumbria, Newcastle upon Tyne, NE1 8ST, UK

*Corresponding authors. E-mail: zgwang@uestc.edu.cn(ZW); richard.fu@northumbria.ac.uk(YF)

Group IVA elements (Si, Ge and Sn) are promising candidates for the anode materials of lithium ion batteries (LIBs) due to their large theoretical specific capacities. However, serious problems of pulverization and capacity degradation resulted from the huge volume changes during charge/discharge operations hindered their successful applications as the anode materials in the LIBs. In this work, diffusion behaviors of Li ions in Si(100) and Si(111) slabs with a piezoelectric field applied perpendicularly to the surfaces were investigated using density functional theory. Results showed that the diffusivity of the Li in Si can be significantly enhanced by applying the electric field generated from the piezoelectric material. This finding can explain well the recent experimental observations in which improved electrochemical performance was obtained using Si/carbon nanotube/BaTiO₃ as the anode for the LIBs. New generation of anode composite materials can be designed based on this idea and the piezoelectric material is used not only to accommodate the volume variation of active materials of Si, but also to enhance the charging rate of the LIBs.

Keywords: Piezoelectric material, Si anode, Lithium ion batteries, Density functional theory

1. Introduction

The relatively low specific capacity of current commercial electrode materials for lithium ion batteries (LIBs) can not satisfy the ever-increasing demands of large energy/power suppliers. Developing new electrode materials and designing their novel structures are critical to improve the cycle life and rate performance and increase the energy density of the LIBs. ^[1] Group IV materials (Si, Ge, and Sn) are promising anode materials for the LIBs due to their large theoretical specific capacities. ^[2] The theoretical specific capacities for Si, Ge and Sn as anodes for the LIBs are 3579, ^[3] 1384, ^[4] and 992 ^[5] mA·h·g⁻¹, respectively, which are larger than that of the currently used commercial graphite anode (372 mA·h·g⁻¹). ^[6] The large capacity densities of the group IV materials come from their capabilities to host more lithium ions to be inserted and extracted, which are generally accompanied with huge volume expansion and contraction. For example, the volume changes of the Si during charging/recharging can be up to 300%. ^[7] The huge volume changes during operation results in pulverization and degradation of the electrical connection between electrodes, ^[8] which becomes the major obstacle for their practical applications.

Tremendous effort has been made to accommodate this volume change, such as reducing the size of active materials to nano-metric levels (e.g. using nanowires, ^[9] nanoparticles, ^[10] nanotubes, ^[11] and hollow nanospheres ^[12]), synthesis of composites with carbon materials (e.g. hollow carbon spheres, ^[13] carbon nanotubes, ^[14] graphene ^[15]), and fabrication of porous structures (e.g. mesoporous Si sponge, ^[16] porous Si nanowires, ^[17] nanoporous silicon networks ^[18]). The extra spaces created using these techniques can be used to mitigate volume expansion/extraction. Therefore, the volume variation can be effectively accommodated and thus the capacity and cycling performance can be improved to some extent. However, these

techniques and associated fabrication methods are either expensive or complicated for a large-scale mass production, and the charge/discharging rate performance of these anode structures cannot satisfy the demands of high power applications.

Designing new structures to accommodate the huge volume changes and improve the rate performance of anode materials with group IV materials is critical for their applications. Integrating a piezoelectric material into the anode materials for the LIBs could be a potential solution for this critical issue. When the piezoelectric material is integrated into the Si anode, the volume changes of the Si upon lithiation can be accommodated by the piezoelectric material through piezoelectric effect. At the same time the piezoelectric potential generated from the piezoelectric material will affect the diffusion of lithium ions inside the Si, as it has been reported that the applied electrical fields can significantly enhance the Li ion diffusion in MoS₂.^[19] Recently, Lee et al.^[20] synthesized Si/carbon nanotube (CNTs)/BaTiO₃ nanocomposite using a high-energy ball-milling process and found that electrochemical performance of the nanocomposite was greatly improved. They attributed this improvement in the increased mobility of Li-ions to the local piezoelectric potentials generated from the BaTiO₃.^[20] Although Lee et al.^[20] simulated the charging/discharging process of Si/carbon nanotube/BaTiO₃ nanocomposite as the anode for LIBs, the mechanisms of the piezoelectric field for the improvement of charging speed have not been clarified, which is crucial for designing new structures of hybrid anode materials for the LIBs. As the Li ions are negatively charged, they could migrate along the direction of the piezoelectric potential much easier than those against or perpendicular to the direction of the piezoelectric potential. Therefore, the direction of piezoelectric potential could strongly affect the Li ion diffusions. However, these have not been systematically investigated so far.

In this work, we studied, for the first time, how the piezoelectric potential affects the Li-ion diffusion in the Si using density functional theory (DFT), and clarified that the enhancement of Li-ion diffusion is dependent on the direction of the piezoelectric potential. The results provide a fundamentally new approach to improve the electrochemical performance of the LIBs when using the group IV materials composites as their anodes.

2. Models

It is well-known that Si(100) and Si(111) surfaces are the two energetically favorable facets of the Si nanocrystals.^[21] These two surfaces possess different surface reconstructions. At room temperature, the Si(100) surface exhibits a 2×1 reconstruction, whereas the Si(111) surface shows a 7×7 reconstruction.^[22] We used periodical slabs consisting of 18 and 10 atomic layers to model the Si(100) and Si(111) surfaces, respectively. The cross- and side-views of ball and stick models of the Si(100) and Si(111) slabs are shown in Fig. 1. A 4×2 buckled-dimer reconstructed Si(100) surface and a dimer-adatom-stacking-fault reconstructed Si(111) surface^[23] were used to represent the Si(100) and Si(111) surfaces, respectively. The 7×7 cell of Si(111) surface was separated into two half unit cells (HUC) by the dimer rows and the corner hole atoms. There were three Si rest-atoms and six Si adatoms in each HUC. The bottom of the slab kept its bulk configuration. Two bottom Si layers were fixed to model the bulk lattice properties, while the other Si atoms were free to relax. The dangling bond of the bottom Si atom was saturated with frozen hydrogen atoms. The unit cells of the Si(100) and Si(111) consisted of $144\text{Si}+16\text{H}$ and $494\text{Si}+49\text{H}$ atoms, respectively. A 25 \AA vacuum space was used to separate the periodic image interactions. The thicknesses of the slab Si(100) and Si(111) were 24.5 and 16.7 \AA , respectively, which were sufficient for the convergence of Li ion diffusion.^[21, 24] A $2\times 4\times 1$

and $2 \times 2 \times 1$ k-point mesh was used for the Brillouin-zone integrations for the Si(100) and Si(111) surfaces, respectively. The diffusion behaviors of the Li ions from Si(100) and Si(111) surfaces into the bulk of Si were studied using the constrain method. [25]

When the Si is used as the anode for the LIBs, large stress is generated due to the volume expansion and contraction upon the lithium insertion and extraction, which causes cracking and pulverization of the Si, then leads to the loss of electrical contact between particles. [8] During the operation of the LIBs, the decomposition of organic electrolyte forms a layer on the Si anode. This layer should be dense and stable, which is also ionically conducting and electronically insulating, however, the large volume change of the Si makes this stable layer difficult to form. [26] Although the nanostructured Si can be used to accommodate this volume change due to its large surfaces, but the surface intercalation is the rate limiting step of lithium intercalation. [21, 24]

Piezoelectric materials can convert mechanical energy into electrical energy and vice versa. The piezoelectric materials can not only accommodate the large volume changes which occur in the Si anodes of the LIBs, but also generate local electric field to enhance the Li mobility. Both Si and piezoelectric materials can be integrated into a suitable matrix such as carbon nanotubes (CNTs). For example, nanostructured Si and piezoelectric materials can be uniformly dispersed in a dense CNTs matrix (see Fig. 2), where the CNTs serve as a matrix providing conducting pathways and also have good adhesion with both Si and piezoelectric materials through surface functioning. A voltage will be produced when the piezoelectric materials are subjected to mechanical strain. The proposed charging process of Si/CNTs/piezoelectric composites is schematically shown in Fig. 2. In a discharged state, there is no strain in the Si and piezoelectric materials as shown in Fig. 2a. Upon lithiation, the volume of the Si expands with insertion of Li ions to form Li_xSi , and the strain caused by this volume expansion is transferred to the

piezoelectric material as shown in Fig. 2b. The piezoelectric material shrinks, and thus can accommodate the volume expansion of Si. Simultaneously an electric potential is generated within the piezoelectric material, therefore, the lithiation process can be enhanced under this piezoelectric potential. The dependence of Li ion diffusion behavior on the strength and direction of electric potentials was investigated in this study. Upon discharging process, the Si contracts whereas the piezoelectric material expands, which can still keep a good electrical contact.

3. Results and Discussion

We firstly examined the adsorption behaviors of Li atoms on Si(100) and Si(111) surfaces. The adsorption energy E_{ads} can be calculated using: ^[27]

$$E_{\text{ads}}(\text{Li}) = E_{\text{slab-Li}} - E_{\text{slab}} - E_{\text{Li}} \quad (1)$$

where $E_{\text{slab-Li}}$ and E_{slab} are the total energies of Si slabs with and without Li adsorption, respectively. E_{Li} is the energy of an isolated lithium atom. The more negative the adsorption energy is, the more energetically favorable the adsorption for the Li ions will be.

The possible adsorption sites of the Li ions in the Si are shown in Fig. 1, and the calculated adsorption energies are listed in Table 1. On the Si(100) surface, various sites of caves (C1 and C2), interdimer (B2), valley bridge (T1), dimer bridge (HB), and pedestal (HH) were considered. According to the calculated adsorption energies, the Li ions prefer to occupy the C1 site. The T3 site is not stable for the Li ion adsorption, thus the Li ion moves to the C1 site after a full relaxation. The B2 site is 0.02 eV less energetically stable than the C1 site for Li ion adsorption. For the Si (111) surface, the various sites of cave (C1), dimer bridge (B), top of hexagon (H1, H2, H3), and other sites (T1, T2, T3) were investigated. The adsorption energy is -2.66 eV for the Li ion adsorbed at the H2 site, which is the most energetically favorable adsorption site.

The diffusion energy barriers of the Li ions in the bulk Si with 64 atoms were calculated using the constrained method. In the bulk Si, the Li ion prefers to occupy the tetrahedral interstitial site, which has four nearest-neighboring Si atoms and six second-nearest-neighboring Si atoms. Diffusion of the Li ion is from one stable position to a neighboring position by passing through a hexagon space.^[28] The calculated diffusion energy barrier is 0.56 eV, which agrees well with the value of 0.57 eV calculated using climbing-image nudged elastic band (CI-NEB) method reported in literature.^[29]

The diffusion of the Li ion from the the most stable adsorption sites, i.e. C1 site in Si(100) and H2 site in Si(111), to the inner sites of the slabs was calculated using the constrained method. The diffusion energy profiles for the Li ions into the Si(100) and Si (111) are shown in Figs. 3a and 3b, respectively. The insets show the corresponding diffusion paths. The diffusion energy barriers are 1.53 and 1.69 eV for the Li ions to diffuse from Si(100) and Si (111) surfaces into the sub-surfaces, respectively. The larger values of both adsorption energy barrier and diffusion energy barrier of the Li ion in the Si (111) surface compared with those in the Si(100) surface indicate that the Li intercalation is easier to occur on Si(100) surface than Si(111) surface. Our simulation results clearly explain why the mean residence time of the Li on the Si (111) is longer than that on the Si(100) surface which was experimentally observed in the literature.^[30]

Results also showed that the diffusion energy barrier of the Li ions through the surface is larger than that diffusing inside the slab. For examples, the diffusion energy barrier is 1.55 eV for the Li through the Si(100) surface, whereas it is in the range between 0.58 and 0.65 eV inside the slab, which means that Li diffusion from the Si(100) and Si(111) surfaces is energetically unfavorable for surface intercalation. It was reported that surface modifications of Si with P or Al doping can reduce the diffusion energy barrier through the Si(100) and Si(111) surfaces.³³

After understanding the diffusion of Li ions in the Si(100) and Si(111), we then further investigated effects of the generated electric potential on the Li ion diffusion after the piezoelectric field was applied perpendicularly to the surface. We defined that the piezoelectric field penetrating through the surface with an outward direction has a positive value and the one with an inward direction has a negative value. We have analyzed different situations through initial tests and concluded that the electric field has significant influences on the diffusion behavior when its direction is perpendicular to the surface of Si. Therefore, in this paper, we focused on two situations in which the electric field was along inward and outward directions through the surface, respectively. A saw-tooth potential profile perpendicular to the surface as described in reference [31] was used to model the electric field. The obtained diffusion energy profiles of the Li ions diffused into Si(100) and Si (111) with the applied piezoelectric fields of -0.5 – 0.5 V/Å are shown in Figs. 3a and 3b, respectively, and the corresponding diffusion paths are also shown in the insets in Fig. 3. The piezoelectric potential indeed has an apparent effect on the diffusion behaviors of Li ions. Negative piezoelectric potential can assist the Li diffusion, whereas the positive one will retard the diffusion. Figs. 3c and 3d show the changes of diffusion energy barriers (ΔE) as a reference to the ones without piezoelectric fields for the Li ions diffusing into the Si(100) and Si (111) along the paths as shown in the insets of Figs. 3a and 3b, respectively. The positive and negative values means the increase and decrease of the diffusion energy barriers, respectively. As can be seen from the figures, the diffusion energy barriers decrease with the negative piezoelectric potential but increase with the positive one. The larger the applied piezoelectric potential is, the larger the increased or decreased values of diffusion energy barrier will be. For example, the value of ΔE for Li diffusion in Si(100) surface decreases

to 0.31 eV and increases to 0.57 eV with applied values of negative and positive piezoelectric potentials of 0.5 V/Å, respectively.

The piezoelectric potential also shows a significant influence on the diffusion of Li atoms from the surface to the subsurface of the Si when compared with that of diffusion inside the bulk Si. For example, the diffusion energy barrier decreases with values of 0.31 and 0.06 eV for the Li ion diffusion from site 0 to site 1 and from site 3 to site 4 in the Si(100) slab, respectively (see Fig. 3). The diffusivity (D) varies exponentially with the diffusion energy barrier (E_A) through the relationship of: ^[32]

$$D \propto e^{-E_A/k_B T} \quad (2)$$

in which T is temperature and k_B is Boltzmann constant. The change value of 0.06 eV seems very small, but from the above equation, an increase or decrease of 0.06 eV will induce the diffusivity change by a factor of ~ 10 ($e^{0.06/300k_B} = 10$) at room temperature. As discussed above, the Li diffusion from the surface to the subsurface is the main process delaying the diffusivity of Li ion in Si. By applying the generated piezoelectric potential, the diffusion energy barriers are reduced significantly, i.e. 0.31 eV and 0.36 eV in Si(100) and Si(111) surfaces with a piezoelectric potential of -0.5 V/Å. Based on equation (1), the diffusivity can be improved $\sim 10^5$ and $\sim 10^6$ times when a piezoelectric field of -0.5 V/Å is applied to the Si(100) and Si(111), respectively. **The diffusivity can be improved by $\sim 10^2$ and $\sim 10^3$ times with a small piezoelectric field of -0.1 V/Å in the Si(100) and Si(111), respectively.** The results can explain well the experimental observation of significantly reduced charging time for the Si anode after applying the BaTiO₃ piezoelectric materials. ^[20]

The piezoelectric materials can be used to accommodate the volume changes of active materials of Si, and the piezoelectric potential generated from the piezoelectric materials can

affect the diffusivity of Li ions in the Si. A negative piezoelectric potential, i.e. the orientation of electric potential is along the diffusion path, can enhance the diffusion, whereas a positive one will prevent the diffusion. Therefore, by suitably designing of the Si/piezoelectric composites, we could produce new generations of anode materials for the LIBs with the improved electrochemical performance.

4. Conclusion

Effects of piezoelectric potential on the diffusion of Li ion on the surfaces and inside the Si(100) and Si(111) slabs were investigated using the DFT. The diffusion can be enhanced or reduced by applying the piezoelectric potentials, which depends on the directions of the applied piezoelectric potentials. The diffusion barriers decrease with increasing the strength of the piezoelectric field when its direction is along the diffusion path. The diffusion from the surface to the subsurface is identified as the main process controlling the diffusivity of Li ion in Si surfaces. The diffusion barriers are significantly reduced as the existence of piezoelectric field and the diffusivity can be improved $\sim 10^5$ - 10^6 times with an applied piezoelectric field of -0.5 V/Å for the surface diffusion.

Simulation methods

The DFT calculations were performed using SIESTA code, ^[33] which employed a linear combination of numerical localized atomic orbital basis sets to describe the valance electrons and norm-conserving nonlocal pseudopotentials to describe atomic core. ^[34] Double- ζ basis set plus polarization functions were used to describe the electron state. In the simulations, generalized gradient approximation (GGA) and Perdew-Burke-Ernzerhof (PBE) exchange and correlation

functions were used. ^[35] An energy mesh cutoff of 200 Ry was used to calculate the Hamiltonian matrix elements.

Acknowledgement:

This work was financially supported by the National Natural Science Foundation of China (11474047). Funding supports from UK EPSRC EP/P018998/1 and Royal academy of Engineering UK-Research Exchange with China and India are also acknowledged. This work was carried out at National Supercomputer Center in Tianjin, and the calculations were performed on TianHe-1(A).

References:

- [1] a) A. S. Arico, P. Bruce, B. Scrosati, J.M. Tarascon, W. van Schalkwijk, *Nat. Mater.* **2005**, *4*, 366-377; b) X. Wang, Q. Weng, Y. Yang, Y. Bando, D. Golberg, *Chem. Soc. Rev.* **2016**, *45*, 4042-4073.
- [2] a) L. Ji, Z. Lin, M. Alcoutlabi, X. Zhang, *Energ. Environ. Sci.* **2011**, *4*, 2682-2699; b) X.L. Wu, Y.G. Guo, L.J. Wan, *Chem. - An Asian J.* **2013**, *8*, 1948-1958.
- [3] U. Kasavajjula, C. S. Wang, A. J. Appleby, *J. Power Sources* **2007**, *163*, 1003-1039.
- [4] C. Zhang, Z. Lin, Z. Yang, D. Xiao, P. Hu, H. Xu, Y. Duan, S. Pang, L. Gu, G. Cui, *Chem. Mater.* **2015**, *27*, 2189-2194.
- [5] H. Li, X. Huang, L. Chen, *Solid State Ionics* **1999**, *123*, 189-197.
- [6] J. R. Dahn, T. Zheng, Y. H. Liu, J. S. Xue, *Science* **1995**, *270*, 590-593.
- [7] L.F. Cui, Y. Yang, C.M. Hsu, Y. Cui, *Nano Lett.* **2009**, *9*, 3370-3374.
- [8] G. Kim, S. Jeong, J.H. Shin, J. Cho, H. Lee, *ACS Nano* **2014**, *8*, 1907-1912.

- [9] a) S. Jeong, J.P. Lee, M. Ko, G. Kim, S. Park, J. Cho, *Nano Lett.* **2013**, *13*, 3403-3407; b) K. Ogata, E. Salager, C. J. Kerr, A. E. Fraser, C. Ducati, A. J. Morris, S. Hofmann, C. P. Grey, *Nat. Commun.* **2014**, *5*, 3217; c) C. K. Chan, H. Peng, G. Liu, K. McIlwrath, X. F. Zhang, R. A. Huggins, Y. Cui, *Nat. Nano.* **2008**, *3*, 31-35; d) Z. Gan, M. Gu, J. Tang, C.Y. Wang, Y. He, K. L. Wang, C. Wang, D. J. Smith, M. R. McCartney, *Nano Lett.* **2016**, *16*, 3748-3753.
- [10] H. Wu, G. Yu, L. Pan, N. Liu, M. T. McDowell, Z. Bao, Y. Cui, *Nat. Commun.* **2013**, *4*, 1943.
- [11] a) M.-H. Park, Y. Cho, K. Kim, J. Kim, M. Liu, J. Cho, *Angew. Chem.* **2011**, *123*, 9821-9824; b) M.H. Park, M. G. Kim, J. Joo, K. Kim, J. Kim, S. Ahn, Y. Cui, J. Cho, *Nano Lett.* **2009**, *9*, 3844-3847; c) H. Wu, G. Chan, J. W. Choi, I. Ryu, Y. Yao, M. T. McDowell, S. W. Lee, A. Jackson, Y. Yang, L. Hu, Y. Cui, *Nat. Nano.* **2012**, *7*, 310-315.
- [12] Y. Yao, M. T. McDowell, I. Ryu, H. Wu, N. Liu, L. Hu, W. D. Nix, Y. Cui, *Nano Lett.* **2011**, *11*, 2949-2954.
- [13] W.M. Zhang, J.S. Hu, Y.G. Guo, S.F. Zheng, L.S. Zhong, W.G. Song, L.J. Wan, *Adv. Mater.* **2008**, *20*, 1160-1165.
- [14] a) J. Zhou, Y. Lan, K. Zhang, G. Xia, J. Du, Y. Zhu, Y. Qian, *Nanoscale* **2016**, *8*, 4903-4907; b) J. Palomino, D. Varshney, B. R. Weiner, G. Morell, *J. Phys. Chem. C* **2015**, *119*, 21125-21134; c) W.J. Yu, C. Liu, P.X. Hou, L. Zhang, X.Y. Shan, F. Li, H.M. Cheng, *ACS Nano* **2015**, *9*, 5063-5071.
- [15] a) Z. Luo, Q. Xiao, G. Lei, Z. Li, C. Tang, *Carbon* **2016**, *98*, 373-380; b) K. Feng, W. Ahn, G. Lui, H. W. Park, A. G. Kashkooli, G. Jiang, X. Wang, X. Xiao, Z. Chen, *Nano Energy* **2016**, *19*, 187-197.

- [16] X. Li, M. Gu, S. Hu, R. Kennard, P. Yan, X. Chen, C. Wang, M. J. Sailor, J.G. Zhang, J. Liu, *Nat. Commun.* **2014**, *5*, 4105.
- [17] Y. Chen, L. Liu, J. Xiong, T. Yang, Y. Qin, C. Yan, *Adv. Func. Mater.* **2015**, *25*, 6701-6709.
- [18] J. Zhu, C. Gladden, N. Liu, Y. Cui, X. Zhang, *Phys. Chem. Chem. Phys.* **2013**, *15*, 440-443.
- [19] W. Shi, Z. Wang, Z. Li, Y. Q. Fu, *Mater. Chem. Phys.* **2016**, *183*, 392-397.
- [20] B.S. Lee, J. Yoon, C. Jung, D. Y. Kim, S.Y. Jeon, K.H. Kim, J.H. Park, H. Park, K. H. Lee, Y.S. Kang, J.H. Park, H. Jung, W.R. Yu, S.G. Doo, *ACS Nano* **2016**, *10*, 2617-2627.
- [21] B. Peng, F. Cheng, Z. Tao, J. Chen, *J. Chem. Phys.* **2010**, *133*, 034701.
- [22] D. J. Eaglesham, A. E. White, L. C. Feldman, N. Moriya, D. C. Jacobson, *Phys. Review Lett.* **1993**, *70*, 1643-1646.
- [23] D. Vanderbilt, *Phys. Rev. B* **1987**, *36*, 6209-6212.
- [24] S. C. Jung, Y.K. Han, *Phys. Chem. Chem. Phys.* **2011**, *13*, 21282-21287.
- [25] X. Sun, Z. Wang, Y. Q. Fu, *Sci. Rep.* **2015**, *5*, 18712.
- [26] H. Wu, Y. Cui, *Nano Today* **2012**, *7*, 414-429.
- [27] E. Lee, K. A. Persson, *Nano Lett.* **2012**, *12*, 4624-4628.
- [28] Z. Wang, Q. Su, H. Deng, W. He, J. Lin, Y. Q. Fu, *J. Mater. Chem. A* **2014**, *2*, 13976-13982.
- [29] a) V. Milman, M. C. Payne, V. Heine, R. J. Needs, J. S. Lin, M. H. Lee, *Phys. Rev. Lett.* **1993**, *70*, 2928-2931; b) W. H. Wan, Q. F. Zhang, Y. Cui, E. G. Wang, *J. Phys.-Condes. Matter* **2010**, *22*, 415501; c) G. A. Tritsarlis, K. J. Zhao, O. U. Okeke, E. Kaxiras, *J. Phys. Chem. C* **2012**, *116*, 22212-22216.

- [30] H. Kleine, M. Eckhardt, D. Fick, *Surf. Sci.* **1995**, 329, 71-76.
- [31] J. Neugebauer, M. Scheffler, *Phys. Rev. B* **1992**, 46, 16067-16080.
- [32] G. H. Vineyard, *J. Phys. Chem. Solids* **1957**, 3, 121-127.
- [33] J. M. Soler, E. Artacho, J. D. Gale, A. Garcia, J. Junquera, P. Ordejon, D. Sanchez-Portal, *J. Phys.-Condens. Mat.* **2002**, 14, 2745-2779.
- [34] N. Troullier, J. L. Martins, *Phys. Rev. B* **1991**, 43, 1993-2006.
- [35] J. P. Perdew, W. Yue, *Phys. Rev. B* **1986**, 33, 8800-8802.

Table 1 Calculated adsorption energies (eV) for Li ion on Si(100) and Si (111) surfaces

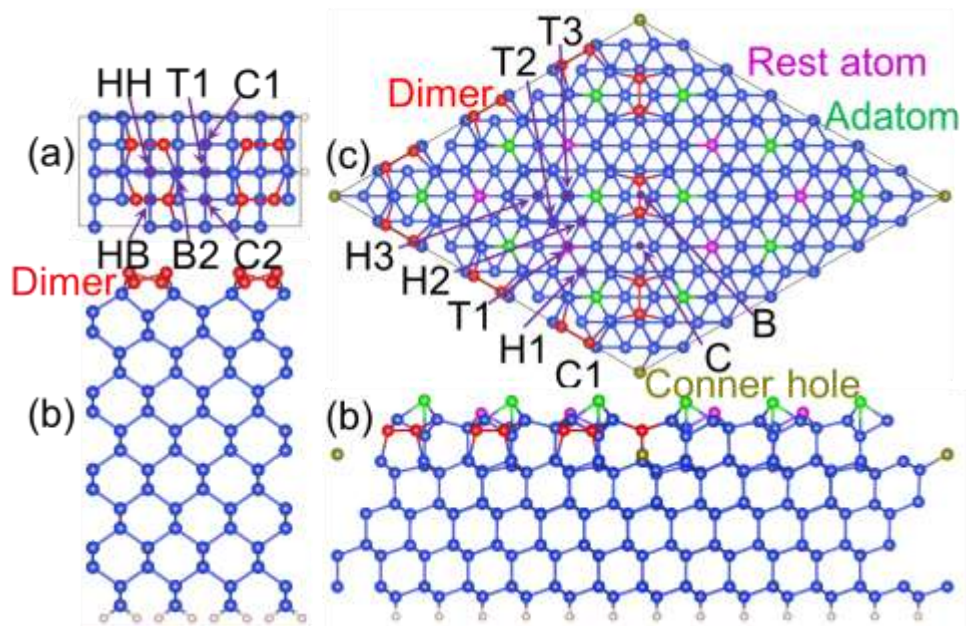
Si(100)	B2	HB	HH	T1	C1	C2		
	-2.30	-1.78	-2.00	-2.31	-2.32	-1.81		
Si(111)	B	C	H1	H2	H3	T1	T2	T3
	-1.66	-1.96	-2.65	-2.66	-1.90	-2.19	-2.19	-1.87

Figure captions:

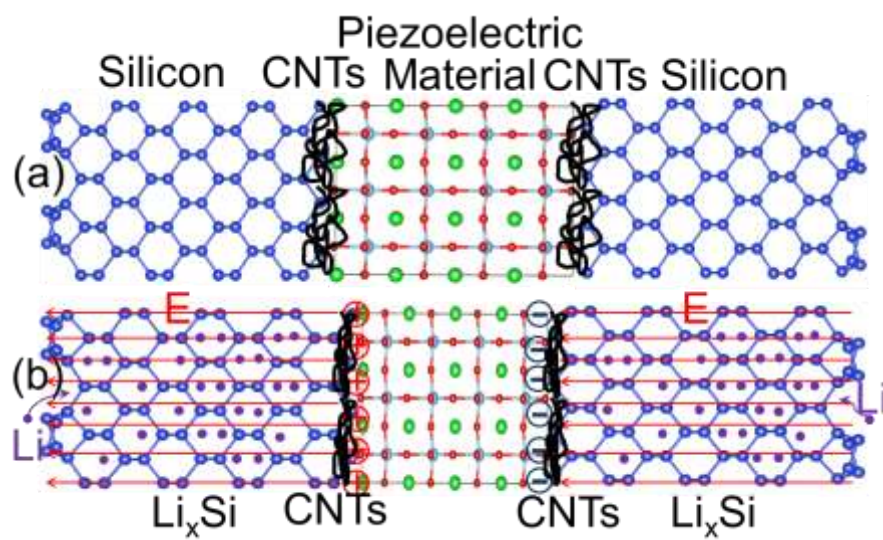
Figure 1 The cross- and side-views of ball and stick models of (a)/(b) Si(100)-(4×2) and (c)/(d) Si(111)-(7×7) slabs. The possible adsorption sites are also shown.

Figure 2 Schematic illustrations of charging processes of Si/Piezoelectric composites. (a) At the discharged state there is no strain in the piezoelectric materials. (b) During charging the strain caused by the volume expansion of Si upon lithiation is transferred to piezoelectric material. Meanwhile piezoelectric field is generated at the Si anode, which can affect the diffusion of Li ion.

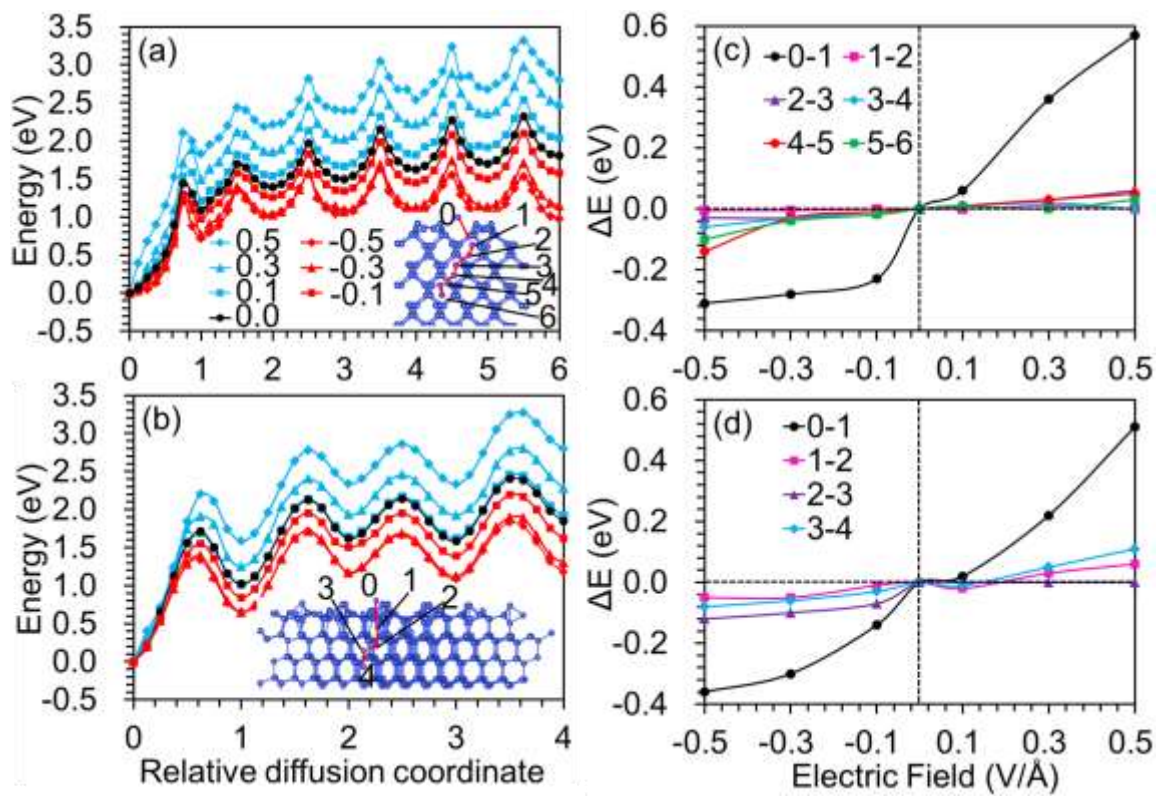
Figure 3 Diffusion energy profiles for Li ion into (a) Si(100) and (b) Si (111) with the applied piezoelectric fields of $-0.5-0.5 \text{ V/\AA}$. Insets show the diffusion paths from the surface to the inside. Changes of diffusion energy barriers (ΔE) as a reference to the one without piezoelectric field as Li ions diffuse into (c) Si(100) and (d) Si (111). Symbol of 0-1 represents Li ion diffusion from site 0 to site 1.



Wang and Fu, Figure 1



Wang and Fu, Figure 2



Wang and Fu, Figure 3